**THE 25 MARCH 2020 TSUNAMI AT THE KURIL ISLANDS: ANALYSIS AND NUMERICAL SIMULATION****Andrey Zaytsev^{1,2}, Guney G. Dogan³, Grigory Dolgikh⁴, Stanislav Dolgikh⁴, Ahmet C. Yalciner³ and Efim Pelinovsky^{2,5}**¹ *Special Research Bureau for Automation of Marine Researches, Yuzhno-Sakhalinsk, Russia*² *Nizhny Novgorod State Technical University n.a. R.E. Alekseyev, Nizhny Novgorod, Russia*³ *Middle East Technical University, Ankara, Turkey*⁴ *V.I. Ilichev Pacific Oceanological Institute, Vladivostok, Russia*⁵ *Institute of Applied Physics, Nizhny Novgorod, Russia***ABSTRACT**

A strong earthquake with a magnitude of 7.5 occurred near the island of Paramushir (Kuril Islands) on 25 March 2020. It caused a weak tsunami in Kamchatka and the Kuril Islands. Earthquake and tsunami data from three DART buoys are discussed and compared with numerical simulations. It is shown that the calculated and measured tsunami characteristics on the DART buoys is in very good agreement. There are also data on the recording of this earthquake by a laser strain-meter installed in the Sea of Japan at Shults cape at a distance of more than 2,000 km from the epicenter of the earthquake. There is also an instrumental recording of the tsunami at the Vodopadnaya point in the southeast of Kamchatka. Unfortunately, there was a large storm at sea at this time, and the amplitudes of tsunami waves and storm waves were comparable to each other, so here the agreement between calculations and observations does not seem good enough.

Key words: *tsunami, numerical simulation, laser strain-meter, shallow-water equations, tsunami observations*

1. INTRODUCTION

On 25 March 2020, at 02:49 GMT (05:49 Moscow time), a strong earthquake occurred east of the Kuril Islands near Paramushir Island with $M = 7.5$. The epicenters of the earthquake and intensity contours on a 12-point scale are MSK-64 shown in Fig. 1. It caused a tsunami on a number of islands of the Kuril ridge and was also recorded by DART buoys (their locations are shown in Fig. 1). The earthquake was also recorded by laser strain-meters at Shults cape in the Sea of Japan (Figure 1), and the tsunami was instrumental at the Vodopadnaya station in southeast Kamchatka (Figure 1). The present work presents available data on earthquake and tsunami, as well as numerical simulation of the tsunami.

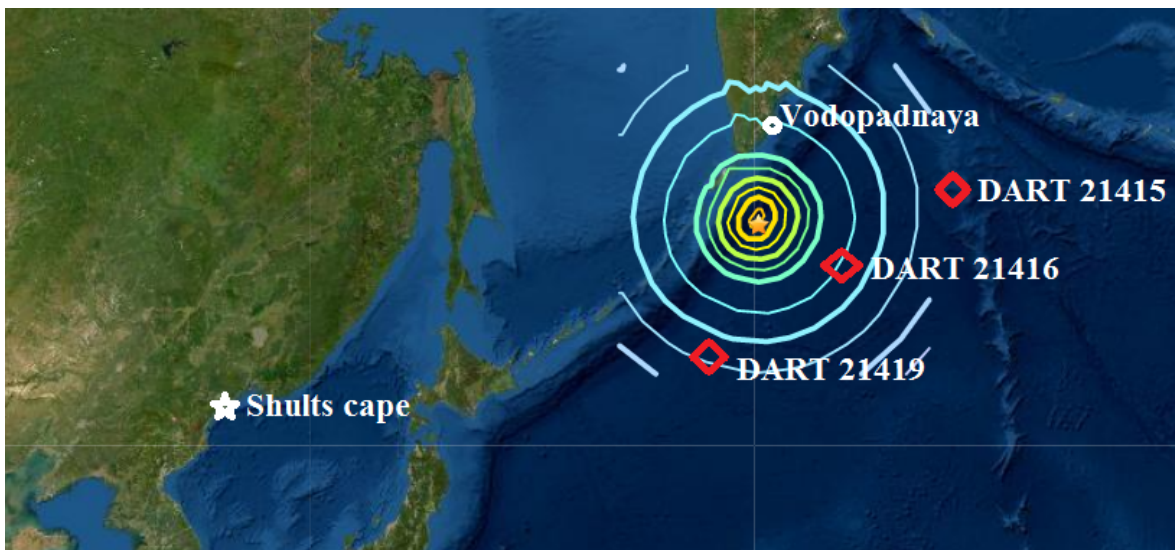


Fig. 1. The epicenter of the 25th March 2020 earthquake with intensity circuits, as well as the position of the DART buoys

It should be noted that catastrophic tsunamis previously occurred in this area, especially note the tsunami of November 4, 1952, which led to the death of several thousand people [[Gordon A. Macdonald and Chester K. Wentworth, 1954](#)]. In the north of the Kuril Islands and on the Kamchatka Peninsula, Chilean tsunamis of 1960, 2010 and 2015 were recorded [Liu et al, 1994]. Therefore, the analysis of developments in this area has an undeniable scientific and practical interest.

2. EARTHQUAKE AND TSUNAMI RECORDING

In Russia, earthquake parameters were determined in the Service of Urgent Reports (SSD) of the Federal Research Center "Unified Geophysical Service of the Russian Academy of Sciences" (FIC EGS RAS) in Obninsk using station data obtained from digital seismic stations

of Russia, CIS countries and abroad [http://www.ceme.gsras.ru/cgi-bin/new/quake_stat.pl?sta=20201185&l=0] (USGS data will be listed in the next section.) An urgent message about this earthquake 11 minutes after its occurrence was transmitted to the operational duty officer of the Russian Emergencies Ministry. According to eyewitnesses [<https://sakhalin.info/news/186919>] in Severo-Kurilsk (Paramushir Island), the tsunami wave arrived at 15:15 local time (4:15 GMT); its height, determined visually, was about 50 cm. There were no casualties and destruction. According to information from the post of UGMS Sakhalin in the city of Severo-Kurilsk (Fr. Paramushir), the first tsunami wave arrived at 15:04 local time with a height of 40 cm. the second wave came after 50 minutes and a third wave arrived after another 60 minutes. It is worth noting that at this time, a cyclone passed over the region, and there was a storm at sea, but against the background of the storm, large waves stood out clearly, which everyone seemed to be a tsunami.

Instrumentally, waves were recorded at the Vodopadnaya sea level measurement station, the Russian Tsunami Warning Service. The station is located on the southeastern coast of the Kamchatka Peninsula and has coordinates: 51.833 °N., 158.067 °E [<http://rtws.ru/sea-level/vodopodnaya>]. According to the analysis of the record, large waves that differ from background waves are observed 45 minutes after the earthquake, which coincides with the calculation results presented below (Figure 2).

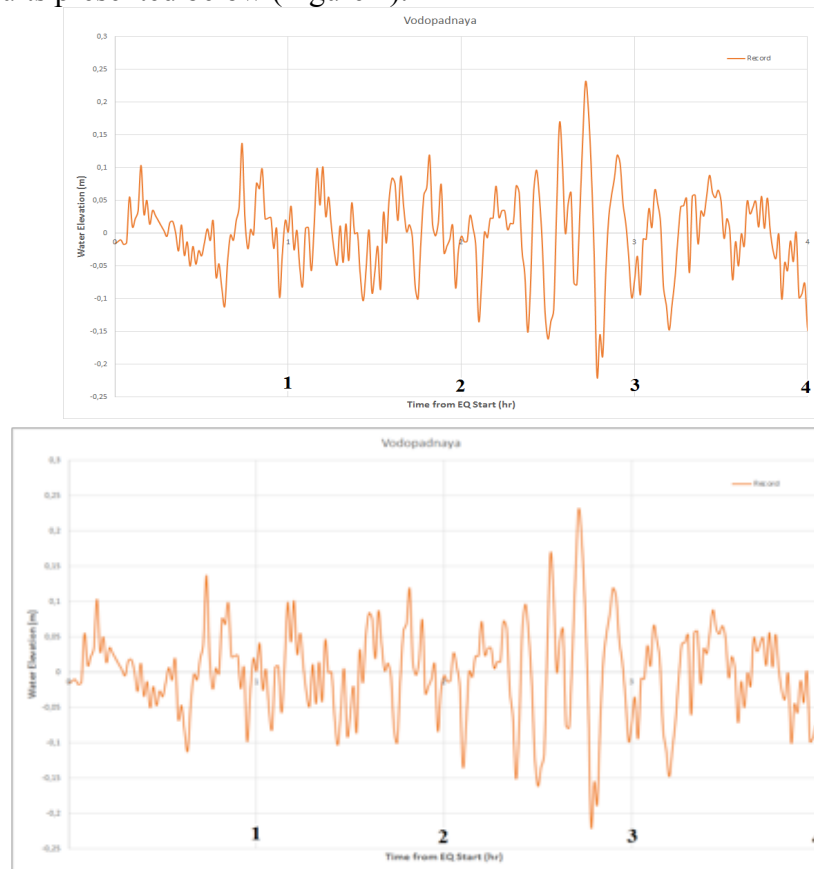


Fig. 2 Record of tsunami waves (orange line) at the point "Vodopadnaya" station

The earthquake and the strain jump associated with the movements of the seabed in the center of tsunami formation were also recorded by a laser strain-meter installed at the marine experimental base of POI FEB RAS "C. Shults," at coordinates 42.58 N 131.157 E at a distance of almost 2150 km from the epicenter (Kuril Island). Figure 3 shows the processed recording of a laser strain-meter with a measuring length of 52.5 meters and a north-south orientation. To isolate variations in the micro deformations of the earth's crust caused by a tsunamigenic earthquake, variations in the micro deformations of the earth's crust caused by fluctuations in atmospheric pressure were subtracted from the laser strain-meter data, as described in [Dolgikh et al. 2020] Based on the experience of recording past earthquakes and tsunamis [Dolgikh et al. 2007, Zaytsev et al, 2019], it was possible to talk about a possible tsunami hazard. On the recording of the laser strain-meter, the earthquake was recorded at 02:53 GMT and after 4 minutes the beginning of the deformation anomaly that caused the tsunami was recorded. And already 15 minutes after the start of the earthquake, it was possible to talk about the occurrence of a tsunami.

Fluctuations of the bottom during the earthquake and tsunami were also recorded by the DART buoy system shown in Figure 1 (these records will be shown below compared to the results of the numerical simulation).

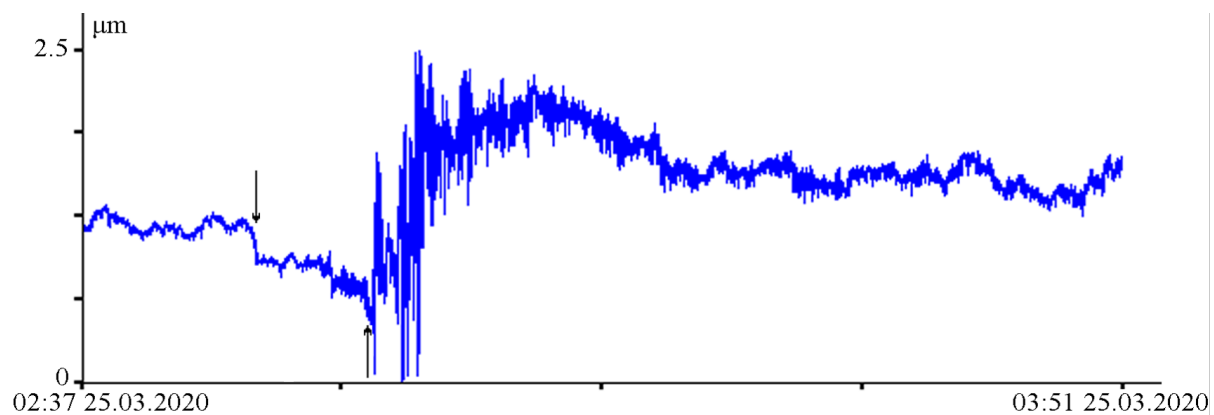


Fig. 3 Processed recording of laser strain-meter signal. The down arrow shows the time of the earthquake, the up arrow shows the registration of deformation movement, showing the beginning of tsunami

3. NUMERICAL TSUNAMI SIMULATION

To numerically simulate the tsunami on 25th March 2020, we used data from the US Geophysical Service [<https://earthquake.usgs.gov/earthquakes/eventpage/us70008fi4/finite-fault>]. The coordinates of the epicenter are 49.0°N, 157.7°E and the focal depth is 57 km. Figure 4 shows the surface projection of the sliding distribution superimposed on the GEBCO bathymetry. Thick white lines indicate the main boundaries of the plates [Bird, 2003]. The figure shows the shear distribution (slip) along the fault. As can be seen from Figure 4, this

value varies from 1 to 4 m. In our calculations, we used the value of 2.5 m. The fault length is 80 km; the fault width is 30 km, the angle between the meridian and the fault line (strike angle) is 204° , the angle of incidence (dip angle) is 48° and the angle of movement (rake angle) is 89° .

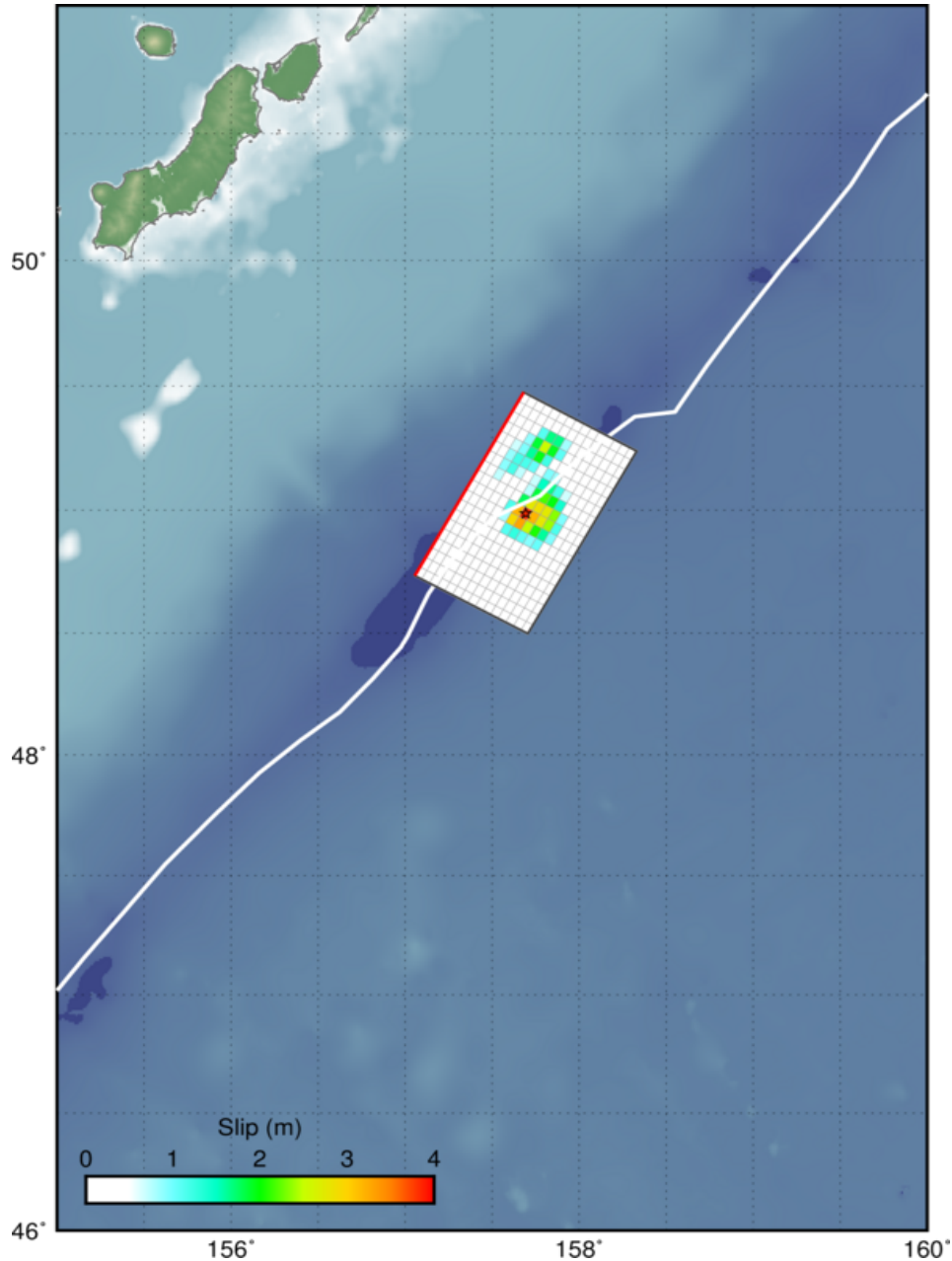


Fig. 4. Surface projection of sliding distribution superimposed on GEBCO bathymetry. Thick white lines indicate the main boundaries of the plates [Bird, 2003]. Gray circles, if any, are the locations of aftershocks

Using the available earthquake information, the initial displacement of sea level at the time of the earthquake is calculated according to the Okada formulas [Okada, 1985]. The maximum increase in the water level in the center is 25 cm and the decrease in the level is 4 cm. The propagation of tsunami waves was carried out using the NAMI-DANCE computational complex [Zaytsev et al. 2019; Zaytsev et al. 2016], solving the system of equations of shallow water in spherical coordinates on the rotating Earth taking into account the friction force.

$$\frac{\partial M}{\partial t} + \frac{1}{R \cos \theta} \frac{\partial}{\partial \lambda} \left(\frac{M^2}{D} \right) + \frac{1}{R \cos \theta} \frac{\partial}{\partial \theta} \left(\frac{MN \cos \theta}{D} \right) + \frac{gD}{R \cos \theta} \frac{\partial}{\partial \lambda} +$$

$$+ \frac{gn^2}{D^{7/3}} M \sqrt{M^2 + N^2} = fN, \tag{1}$$

$$\frac{\partial N}{\partial t} + \frac{1}{R \cos \theta} \frac{\partial}{\partial \lambda} \left(\frac{MN}{D} \right) + \frac{1}{R \cos \theta} \frac{\partial}{\partial \theta} \left(\frac{N^2 \cos \theta}{D} \right) + \frac{gD}{R} \frac{\partial}{\partial \theta} +$$

$$+ \frac{gn^2}{D^{7/3}} N \sqrt{M^2 + N^2} = -fM, \tag{2}$$

$$\tag{3}$$

$$\frac{\partial \eta}{\partial t} + \frac{1}{R \cos \theta} \left[\frac{\partial M}{\partial \lambda} + \frac{\partial}{\partial \theta} (N \cos \theta) \right] = 0,$$

where η – the displacement of the water surface, t - time, M and N - the components of water flow along longitude λ , and latitude θ , f - the Coriolis parameter ($f = 2\Omega \sin[\theta]$) and $[\omega]$ is the rotation speed of the Earth. (rotation period 24 hour), R - Earth radius, $D = h(x, y) + \eta$ – the total depth of the basin and $h(x, y)$ is the unperturbed depth of the water, g is the gravitational constant, n is the roughness coefficient of the bottom (the so-called Manning formula). We took $n = 0.015 \text{ m}^{-1/3}\text{s}$, which is characteristic of the natural bottom (sand, fine pebbles).

For modeling, a bathymetry data, which was obtained from the 30-second bathymetry of the World Ocean (GEBCO30 Digital Atlas) including more accurate coastal bathymetry of the Kuril Islands, which was obtained from various sources of navigation charts, was used. The grid size used in the simulations is 500 m. Numerical modeling was carried out for 6 hours. Completely reflecting boundary conditions were adopted on the shore, and conditions for the free departure of waves on the morph. The distribution of the maximum wave amplitudes for the entire calculation time is shown in Figure 5. The main impact of the tsunami falls on the island of Paramushir.

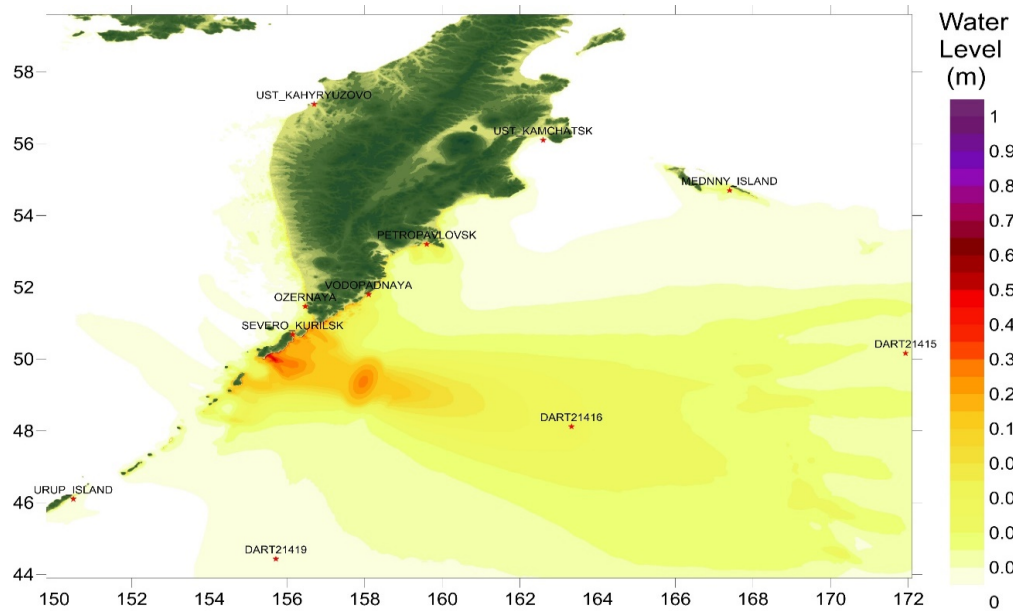


Fig. 5 Distribution of computed maximum water surface elevations during tsunami of 25th March 2020

The tsunami was recorded at several stations. The Deep Sea Tsunami Detection Station (DART 21415, Figure 1) with coordinates 50.164 N, 171.934 E. (50 ° 9 '51 "N 171 ° 56' 4" E), installed at a depth of 4811 m, first recorded an earthquake, and after 1 hour 10 minutes, a tsunami. Figure 6 shows the tsunami record and the results of the calculations of wave parameters at this point. The wave heights here are about 1.5 cm, and the period is about 30 minutes. Simulations results show good agreement with the real record.

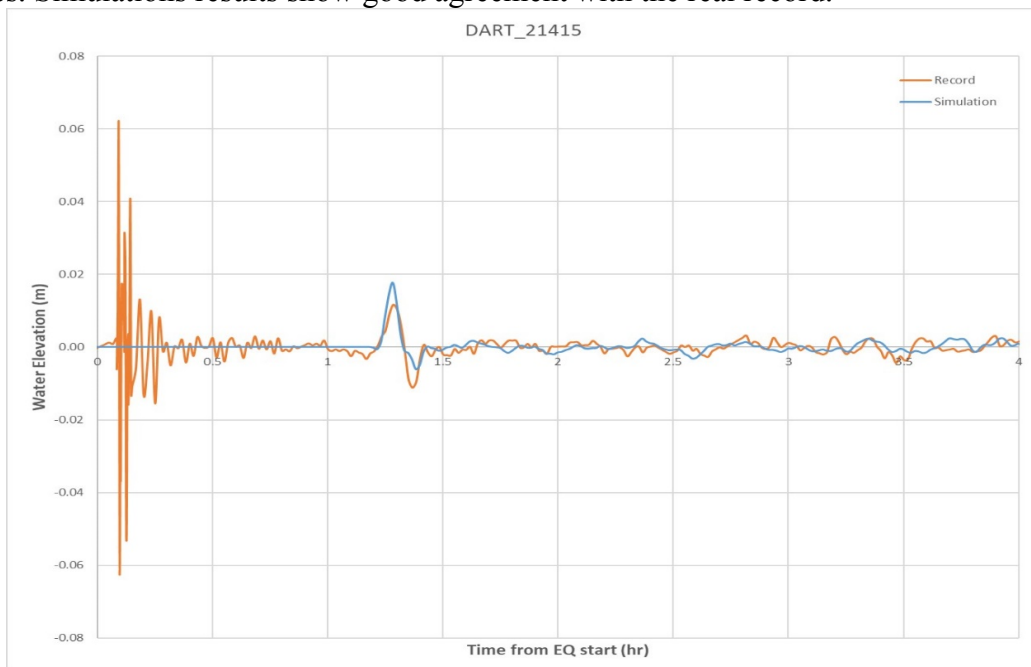


Fig. 6 Recording of tsunami wave 25th March 2020 and calculation results at DART 21415

The Deep Sea Tsunami Detection Station (DART 21416, Figure 1) with coordinates 48.122 N. 163.328 E. (48 ° 7 '18 "N 163 ° 19' 42" E), installed at a depth of 5831 m, and recorded a tsunami 25 minutes after the earthquake. Figure 7 shows the tsunami record and calculation results at this point. The maximum wave height is about 4.5 cm and a period of about 20 minutes. A good agreement of calculations with measurements is also obtained at this location.

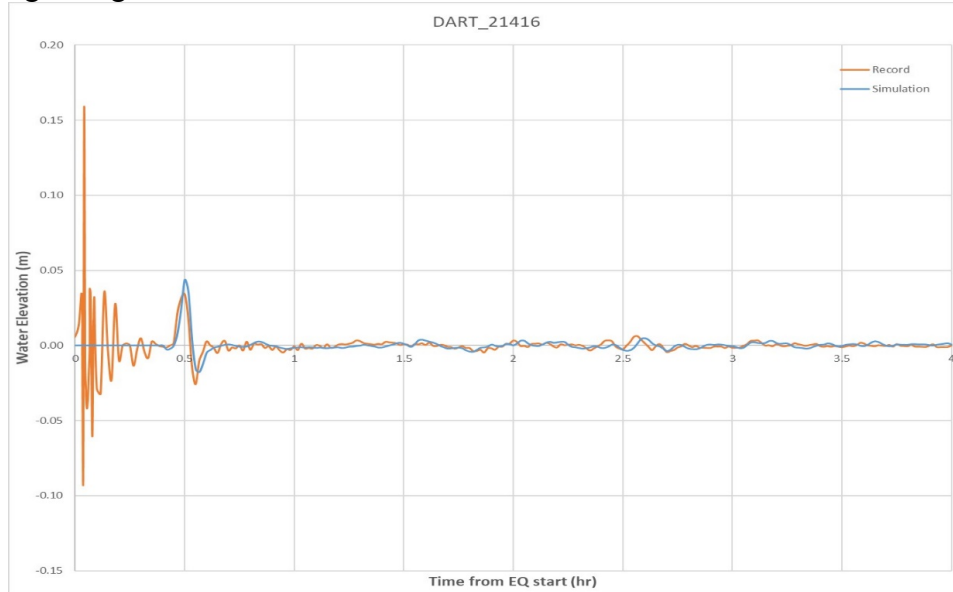


Fig. 7 Recording of tsunami wave 25th March 2020 and calculation results at DART 21416

The Deep Sea Tsunami Detection Station (DART 21419, Figure 1) with coordinates 44.435 N. 155.717 E (44 ° 26 '6 "N 155 ° 43' 0" E), installed at a depth of 5282 m, and recorded a tsunami 35 minutes after the earthquake noises remains unclear.

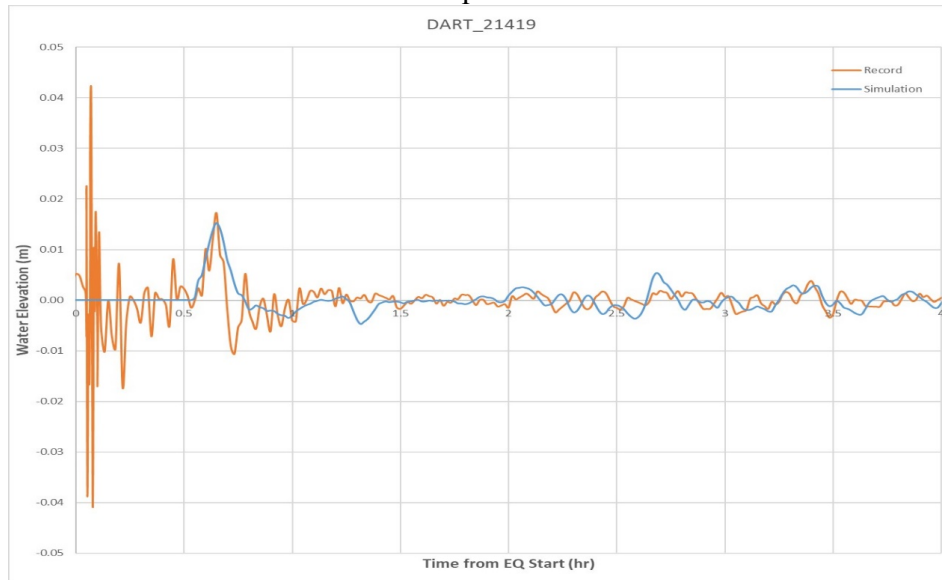


Fig. 8 Recording of tsunami wave 25th March 2020 and calculation results at DART 21419

Figure 8 shows the tsunami record and calculation results at this point. The maximum wave height is calculated as 1.6 cm and a period of about 35 minutes is obtained. Calculations show good agreement with the real record, which, however, is noisy, unlike records on other DART buoys.

Figure 9 shows the comparison of the calculation results with the tsunami record at the Vodopadnaya station). The agreement of these calculations with observations is not very good since, as already indicated, there was a storm at sea on this day, and the waves were significant. Relatively good agreement is observed for the first wave both in terms of arrival and in terms of wave height. A particularly large difference is observed 2.5 hours after the earthquake. The nature of such large waves can be related to both storm conditions and possible interference of tsunami waves arriving in the design area after reflection from the coast outside the design area. Currently, we do not have enough information to explain the appearance of large waves a few hours after the earthquake.

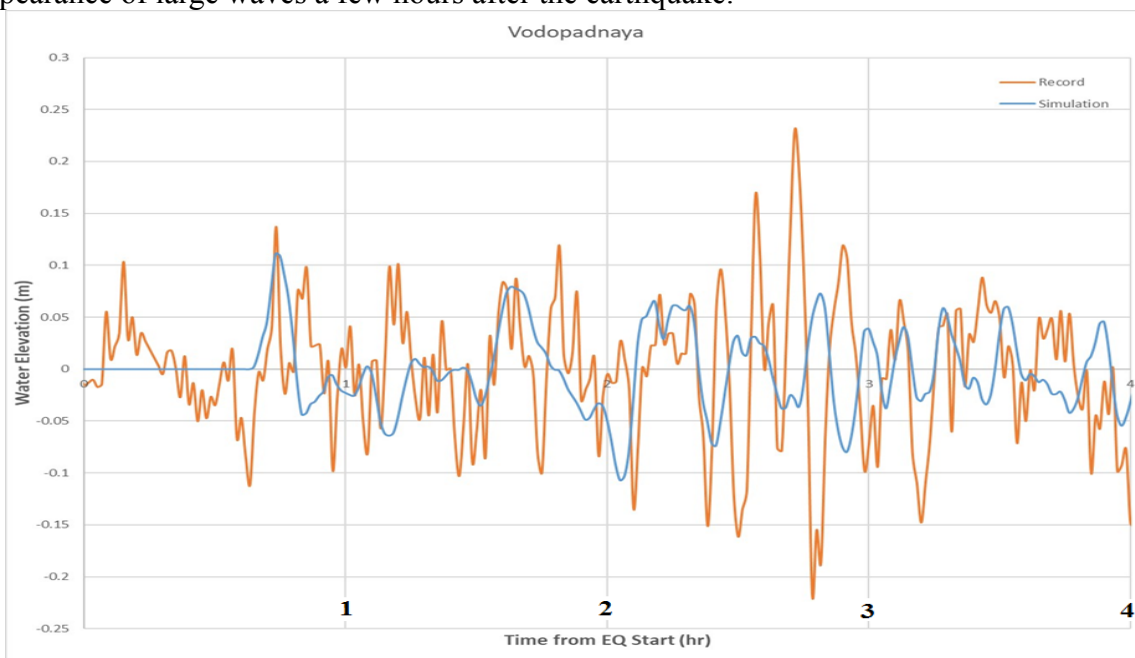


Fig. 9. Recording of tsunami waves (orange line) and calculation results (blue line) at the point "Vodopadnaya" station

4. CONCLUSIONS

On March 25, a strong earthquake with a magnitude of 7.5 near the island of Paramushir (Kuril Islands) caused a weak tsunami in Kamchatka and the Kuril Islands. The event was recorded by three DART buoys and a laser strain-meter installed in the Sea of Japan at Shults cape. We present the instrumental data on the recording of the earthquake and the tsunami. Using the shallow water theory, numerical modeling of the tsunami on 25th March 2020 was carried out. Comparison of the simulation results with tsunami records at deep-sea

DART stations show very good agreement. On the other hand, the agreement between the instrumental recording of the tsunami in the southeast of Kamchatka was not very good, since at that time, a storm raged at the sea, and storm waves were comparable to tsunami waves. Nevertheless, the arrival of the first tsunami wave is well reproduced in numerical modeling.

Acknowledgments

The work was partly supported by the subject “Study of the fundamental foundations of the origin, development, transformation and interaction of hydro acoustic, hydro physical and geophysical fields in the World Ocean”, RFBR grants (18-05-80019, 19-55-15005, 20-05-00162) and the grant of the Russian President MD-148.2020.5

REFERENCES

1. **Bird P.** An updated digital model of plate boundaries *Geochemistry Geophysics Geosystems* 2003 Volume 4, 52 pages
2. **Dolgikh G.I., Dolgikh S.G., Kovalev S.N., Koren I.A., Ovcharenko V.V., Chupin V.A., Shvets V.A., Yakovenko S.V.** Recording of deformation anomaly of a tsunamigenous earthquake using a laser strain meter *Doklady Earth Sciences*. 2007. V. 412. № 1. P. 74-76
3. **Dolgikh G.I., Dolgikh S.G., Vasilevskaya L.N., Lisina I.A.** Interaction of the atmosphere and lithosphere in the minute range of periods *Doklady Earth Sciences*. 2020. V. 490. № 1. P. 18-22.
4. **Gordon A. Macdonald and Chester K. Wentworth** The tsunami of November 4, 1952, on the Island of Hawaii *Bulletin of the Seismological Society of America* (1954) 44 (3): 463–469.
5. **Liu, P. L.-F., Cho, Y.-S., Seo, S. N. and Yoon, S. B. (1994)** Numerical Simulation of Tsunami Propagation and Inundation with Application to Hilo, Hawaii, *Technical Report, School of Civil and Environmental Engineering, Cornell University*.
6. **Okada Y.** Simulated empirical law of coseismic crustal deformation *Journal of Physics of the Earth*. 1995. V. 43. P. 697 – 713.
7. **Zaytsev A., Kostenko I., Kurkin A., Pelinovsky E., Yalciner A.** The depth effect of earthquakes on tsunami heights in the Sea of Okhotsk *Turkish J. Earth Sci.* 2016. Vol. 25, N 4. P. 289–299.

8. **Zaytsev, A., Kurkin, A., Pelinovsky, E., Yalciner, A.C.** Numerical tsunami model NAMI-DANCE *Science of Tsunami Hazards*. 2019. V. 38, No. 4. P. 151–168.
9. **Zaytsev A.I., Pelinovsky E.N., Kurkin A.A., Pronin P.I., Yalciner A., Dogan G., Susmoro H., Prasetya G., Hidayat R., Dolgikh G.I., Dolgikh S.G., Zahibo N.** Generation of the 2018 Tsunami on Sulawesi island: possible sources *Doklady Earth Sciences*. 2019. T. 486. № 1. C. 588-592.